SCIENCE CHINA
Physics, Mechanics & Astronomy

• Article •

August 2017 Vol. 60 No. 8: 082011
doi: 10.1007/s11433-017-9032-6

β-decay studies approaching the N=20 island of inversion with a new shell-model Hamiltonian

WeiGuang Jiang, BaiShan Hu, FuRong Xu*, Rui Han, and Hui Hua

School of Physics and State Key Laboratory of Nuclear Physics and Technology, Peking University, Beijing 100871, China

Received March 9, 2017; accepted April 1, 2017; published online May 22, 2017

β-decay properties of N=18-22, Z=10-14 nuclei are analyzed with a new shell-model Hamiltonian using the Gogny density-dependent interaction. The Gogny force which has been widely and successfully used in mean-field theory can provide reasonable two-body matrix elements for cross-shell calculations. The logft values and β-decay level schemes are systematically studied using the D1S-Gogny interaction and compared with the SDPF-M results and experimental data. It is shown that the new Hamiltonian provides reliable results for β-decay along with subtle level schemes for this region. Shell-model calculations with Gogny interaction can lead to a successful description of nuclei in and around the N=20 island of inversion and supplements experiment where sufficient data are not available.

island of inversion, β decay, shell model, Gogny interaction

PACS number(s): 23.40.-s, 21.60.Cs, 21.30.Fe, 21.10.-k

Citation: W. G. Jiang, B. S. Hu, F. R. Xu, R. Han, and H. Hua, β-decay studies approaching the N=20 island of inversion with a new shell-model Hamiltonian, Sci. China-Phys. Mech. Astron. **60**, 082011 (2017), doi: 10.1007/s11433-017-9032-6

1 Introduction

Based on the concept of shell structure established by Mayer [1] in the 1950s, when the number of nucleons reaches the "magic number", nuclei own stable properties such as a spherical ground state (g.s.), a remarkably higher $E(2_1^+)$, and smaller $B(E2)$ than their neighbors. With the development of experimental techniques studies on nuclear physics have been moving towards the drip-line and more exotic characteristics have been uncovered. In the 1970s, the abnormal binding energy of ^{31}Na,^{32}Na, which were tighter than predictions of the spherical shell model, were observed by Thibault et al. [2]. These significantly motivated nuclear physicists and before long further studies had shown a large deformation region around "magic number" N=20 with large $B(E2)$ and low $E(2_1^+)$ [3-5], which deviated strongly from the traditional shell-model prediction. These anomalous properties indicate the quenching of the N=20 shell gap and the probable intrusion of neutron orbits from the pf shell into the sd shell. Warburton et al. [6] proposed that nuclei with intruder ground states would cover the area Z=10-12, N=20-22 with nine candidates. This region is the so-called island of inversion.

In the following years, both theoretical and experimental investigations have been made to understand the microscopic mechanism of inversion and to extend the boundary of the island. During the studies, nuclear theorist found it difficult to explain the abnormal phenomena in this region using traditional shell model and standard model space [7]. To solve these problems, new methods within the shell-model framework, such as the large-scale shell model by Caurier et al. [8], Monte Carlo shell model by Utsuno et al. [9], have been introduced. Despite some discrepancies in predicting the island boundary, all of these methods have concluded that strong sd-pf cross-shell excitations have to be taken into consideration for nuclei around this region. Once the cross-shell

*Corresponding author (email: frxu@pku.edu.cn)

model space is applied, one also needs to construct the proper cross-shell interaction. Effective interactions within one major shell, for example, the PWT interaction [10] for the p shell, USDB interaction [11] for the sd shell and GXPF1 interaction [12] for the pf shell, have been thoroughly investigated and widely used. In most instances, two-body matrix elements (TBMEs) of the effective interactions were originally derived from realistic forces and then modified by fitting experimental data [13, 14] (mainly nuclear binding energies and excitation spectra). However, when the model space contains two or more major shells, the fitting procedure can be very complicated. Not only because of the large number of TBMEs to be fitted, but also there will be large uncertainties in evaluating TBMEs because many of the off-diagonal matrix elements would be insensitive to data fitting.

In the present work, we present a new effective Hamiltonian by introducing a finite-range density-dependent Gogny force [15] in the shell-model frame. The Gogny interaction, which contains 14 free parameters, has been successfully used in mean-field models and has given good descriptions of various properties of nuclei. With this method, the cross-shell TBMEs can be derived naturally. In this paper, we systematically investigate the structure evolution of nuclei in and around the N=20 island of inversion using the Gogny shell model, and develop a unified description about the nuclei in this region. There are other methods that can describe the bulk properties of nuclei in this region [16, 17] but our discussion concentrates on other aspects. In experiments, β-decay is an important tool to study the nuclear structure for neutron-rich nuclei far from stable line. In recent years, more studies have used β-decay as probes for nuclear structure in this region [18-21] because it provides information on correlations between the wave functions of parent and daughter nuclei. In this regard, β-decay properties are carefully discussed in the following context and hopefully bring further understanding for exotic nuclei near N=20.

2 Model

In shell-model calculations with a frozen core, regardless the size of the model space, the effective Hamiltonian [22,23] can always be written as a sum of one- and two-body operators

$$H = \sum_a e_a \hat{n}_a + \sum_{a\leqslant b,c\leqslant d} \sum_{JT} V_{JT}(ab;cd)\hat{T}_{JT}(ab;cd), \tag{1}$$

where e_a is the energy of the single-particle valence orbit and $\hat{n}_a$ is the number operator. The label a denotes quantum numbers (n_a, l_a, j_a).

$$\hat{T}_{JT}(ab;cd) = \sum_{J_z T_z} A^{\dagger}_{JJ_zTT_z}(ab) A_{JJ_zTT_z}(cd) \tag{2}$$

is the two-body density operator for nucleon pairs, which couples to angular momentum J and isospin T.

We consider a Gogny like density-dependent, two-body nucleon-nucleon interaction [15], given by

$$\begin{aligned} V_{NN,12} = &\sum_{i=1}^{2} \mathrm{e}^{-(\boldsymbol{r}_1-\boldsymbol{r}_2)^2/\mu_i^2}(W_i + B_i P^{\sigma} - H_i P^{\tau} - M_i P^{\sigma} P^{\tau}) \\ &+ t_3\delta(\boldsymbol{r}_1-\boldsymbol{r}_2)(1+x_0P^{\sigma})\left[\rho\left(\frac{\boldsymbol{r}_1+\boldsymbol{r}_2}{2}\right)\right]^{\alpha} \\ &+ iW_0\delta(\boldsymbol{r}_1-\boldsymbol{r}_2)(\boldsymbol{\sigma}_1+\boldsymbol{\sigma}_2)\cdot\boldsymbol{k}'\times\boldsymbol{k}. \end{aligned} \tag{3}$$

Here, P^{σ} and P^{τ} are the spin- and isospin-exchange operators, respectively, and ρ is the density of the nucleus. The first two Gaussians provide finite-range attraction between nucleons. The density-dependent term, which originates from three-body correlations, can produce a proper repulsive effect. The last term is a simple spin-orbit coupling, where $\boldsymbol{k}$ and $\boldsymbol{k}'$ are the relative wave vectors of the two nucleons, acting on the right and left sides, respectively.

When we try introducing Gogny forces in the shell model frame, we will have trouble in determining the density distribution $\rho(\boldsymbol{r}_1+\boldsymbol{r}_2)/2$. Driven by the nature of density-dependent force, an iterative calculation is needed. We start with a trial wave function to calculate the density distribution and then diagonalize the Hamiltonian in the whole model space to obtain the approximate solutions. Then the g.s. density is used as new input for the Hamiltonian. The above steps are repeated until convergence. The convergency of this procedure has been tested. With this method, one can acquire TBMEs of the cross-shell model space naturally. To study various properties of nuclei near N=20, a complete set of matrix elements for the sd-pf shell are derived by Gogny interaction. With the TBMEs, the eigen wave functions for the current Hamiltonian can be acquired for cross-shell nuclei in this region, and β-decay observables of interest can be obtained.

As mentioned above, the beta decay can be used as effective probes to investigate the nuclear structure of those neutron-rich nuclei. For allowed transitions in β-decay, there are Fermi (F) and Gamow-Teller (GT) transitions corresponding to different situations in which electron and neutrino have their spins antiparallel and parallel, respectively. The Fermi and GT transition probabilities $B(F)$ and $B(GT)$ are defined as [24]:

$$B(F) = |\langle\psi_f\|\sum_k^A \tau_k\|\psi_i\rangle|^2, \tag{4}$$

and

$$B(GT) = \frac{1}{2J_i+1}|\langle\psi_f\|\sum_k^A \sigma_k\tau_k\|\psi_i\rangle|^2, \tag{5}$$

where $|\psi_i\rangle$ and $|\psi_f\rangle$ describe the states of parent and daughter nuclei, respectively. J_i is the angular momentum of initial state, the index k refers to all nucleons in the many-body system. For a mixed Fermi and GT transition, the ft-value or so-called comparative half-life is

$$ft = \frac{C}{g_v^2 B(F) + g_A^2 B(GT)}, \tag{6}$$

where $C = \frac{2\pi^3\hbar^7 \ln 2}{m_e^5 c^4}$, g_v and g_A are the weak interaction vector and axial-vector coupling constants, respectively. One should note that in the allowed transition $B(F)$ only connects isobaric analogue states. Because of this, for most instances, only the GT transition will occur in β-decay and therefore ft-values calculated with the shell model are actually $ft(GT)$.

3 Discussions and conclusions

In studies of β-decay, we need to relate the theoretical results to the experimental observables, such as the ft value mentioned before. The ft value reflects the order of a transition and allows us to compare the different beta-decay paths independent of decay energies [24]. As the comparative half-life can take a very wide range of values, it is more convenient for us to use the logarithm of the ft value, i.e., $\log ft$.

We performed systematic calculations for Z=10-14, N=18-22 nuclei and detailed information including $\log ft$ are shown in the Table 1 [25]. The results of shell-model calculations using SDPF-M [26,27] and Gogny [28] interactions

Table 1 Experimental and theoretical $\log ft$ values. The calculated shell model results with SDPF-M interaction and D1S-Gogny interactions are both listed. Here Ex are the excitation energies of daughter nuclei, 0 for ground states. The transitions between ground states of parent and daughter nuclei are preferentially shown below. For transitions without exact J^π or no data at all, the corresponding theoretical results shown in the table are with the largest branching ratio. Experimental data are extracted using the NNDC On-Line Data Service[1)], except for data of ^{31}Al→^{31}Si transition, which is taken from ref. [25]

N	^{A}Zi(J^π)	^{A}Zf(J^π)	E_x (MeV)			$\log ft$		
			Expt.	SDPF-M	D1S	Expt.	SDPF-M	D1S
	^{28}Ne(0^+)	^{28}Na(1^+)	0	0	0	4.2	4.49	3.55
	^{29}Na($\frac{3}{2}^+$)	^{29}Mg($\frac{3}{2}^+$)	0	0($\frac{1}{2}^+$)	0	5.06	5.06	4.09
18	^{30}Mg(0^+)	^{30}Al(1^+)	0.69	0.58	2.2	3.96	3.60	3.97
	^{31}Al($\frac{5}{2}^+$)	^{31}Si($\frac{3}{2}^+$)	0	0	0	4.7	4.06	4.64
	^{32}Si(0^+)	^{32}P(1^+)	0	0	0	8.21	4.4	4.3
	^{29}Ne($\frac{3}{2}^+$)	^{29}Na($\frac{5}{2}^+$)	0.07	0.25	0.06	4.76	4.22	3.89
	^{30}Na(2^+)	^{30}Mg(2^+)	1.48	1.69	1.01	5.86	5.23	4.70
19	^{31}Mg($\frac{1}{2}^+$)	^{31}Al($\frac{1}{2}^+$,$\frac{3}{2}^+$)	0.95	1.68($\frac{1}{2}^+$)	1.57($\frac{1}{2}^+$)	6.02	5.17	4.82
	^{32}Al(1^+)	^{32}Si(0^+)	0	0	0	4.36	4.02	3.74
	^{33}Si($\frac{3}{2}^+$)	^{33}P($\frac{1}{2}^+$)	0	0	0	4.96	5.54	4.79
	^{30}Ne(0^+)	^{30}Na(1^+)	0.15	0.34	0.26	4.04	3.93	4.02
	^{31}Na($\frac{3}{2}^+$)	^{31}Mg($\frac{1}{2}^+$)	0	0.17	1.73	4.9	4.43	4.13
20	^{32}Mg(0^+)	^{32}Al(1^+)	0	0.02(1^+)	0.34(1^+)		4.67	4.58
	^{33}Al($\frac{5}{2}^+$)	^{33}Si($\frac{3}{2}^+$)	0	0	0	4.3	4.34	3.74
	^{34}Si(0^+)	^{34}P(1^+)	1.608	0(1^+)	0.35(1^+)	3.35	3.84	4.32
	^{31}Ne($\frac{3}{2}^-$)	^{31}Na		3.35($\frac{5}{2}^-$)	2.14($\frac{5}{2}^-$)		3.98	4.91
	^{32}Na(3^-,4^-)	^{32}Mg(2^-,3^-)	3.04	4.48(2^-)	3.346(2^-)	5	4.75	5.54
21	^{33}Mg($\frac{3}{2}^-$)	^{33}Al($\frac{3}{2}^-$,$\frac{5}{2}^-$)	1.84	5.93($\frac{5}{2}^-$)	2.47($\frac{5}{2}^-$)	5.69	4.67	5.54
	^{34}Al(4^-)	^{34}Si(3^-)	4.26	4.66(4^-)	3.07(3^-)	4.9	4.71	3.93
	^{35}Si($\frac{7}{2}^-$)	^{35}P($\frac{7}{2}^-$)	4.10	4.77($\frac{7}{2}^-$)	2.67($\frac{9}{2}^-$)	>4.6	4.15	4.91
	^{32}Ne(0^+)	^{32}Na		1.52(1^+)	0.70(1^+)		3.81	3.7
	^{33}Na($\frac{3}{2}^+$)	^{33}Mg($\frac{1}{2}^+\frac{3}{2}^+\frac{5}{2}^+$)	0.71	1.54($\frac{3}{2}^+$)	0($\frac{3}{2}^+$)	5.6	4.33	4.37
22	^{34}Mg(0^+)	^{34}Al		0.16(1^+)	0.37(1^+)		4.25	3.50
	^{35}Al($\frac{5}{2}^+$)	^{35}Si($\frac{3}{2}^+$)	0.97	0.62	0.94	4.67	4.16	3.86
	^{36}Si(0^+)	^{36}P(1^+)	1.30	1.16	1.14	4.45	4.2	3.75

1) National Nuclear Data Center Evaluated Nuclear Structure Data File, http://www.nndc.bnl.gov/ensdf/

are shown in the table for comparison. The model space contains all orbits of *sd*-shell ($d_{5/2}$, $s_{1/2}$, $d_{3/2}$) and the first two orbits of *pf*-shell ($f_{7/2}$, $p_{3/2}$) [29, 30]. The SDPF-M interaction is composed of the USD interaction [31] for *sd*-shell, the Kuo-Brown interaction [32] for *pf*-shell, and a modified Millener-Kurath interaction [33] for the cross-shell matrix element. The Gogny interaction, on the other hand, is obtained using the D1S parameter-set [34] without further adjustment and the single particle energies are −3.42, 3.8, −0.91, 9.4 and −9.4 MeV for $d_{5/2}$, $d_{3/2}$, $s_{1/2}$, $f_{7/2}$, $p_{3/2}$, respectively. One should be aware that for initial and final states of the experiment in Table 1, if there are more than one J^π, it means all of them are possible values. A blank space means there is no current experimental data. Most transitions listed in the table are from ground states to ground states. If transitions are forbidden due to selection rules then we present the path from the g.s. of the parent nucleus to the excited state of the daughter nucleus with the largest β-decay branching ratio.

As evident, both interactions reproduce most of the spins and parities of nuclei in their ground states and provide reasonable logft. For N=19-21 isotones, the logft values are in the range of allowed transitions. By analyzing these nuclei with different neutron numbers, as shown in Figure 1, we find that the logft values of transitions grow steadily from Ne to Mg. When going to Al→Si transitions, the logft values of experiment drop dramatically for N=19,21 isotonic chains. For the N=20 chain, both theoretical calculations also show a drop from Z=12 to Z=13. The sudden change in logft values indicates that in the N=19-21 region the wave functions of the ground states in Al deviate from Mg but are more similar to Si. It suggests that Al is a the boundary on the high-Z side of the island of inversion. The experimental half-lives of these nuclei have been studied systematically by Han et al.[2)] and a similar conclusion is drawn. Note that the two theoretical curves give different tendencies for the N=21 isotone chain. This is because these logft values are taken from the g.s. to excited states and it is difficult to determine which theoretical path corresponds to the experimental one as the branching ratios for different paths are close to each other. For N=18 and N=22 isotones, the saltation at Al does not occur and the logft of Mg→Al transitions are much lower than N=19-21 cases.

Besides the overall analysis based on logft, the β-decay schemes can provide more detailed information about the transitions that we are interested in. While we try to study β-decay schemes within the shell-model frame, both wave functions of the parent and daughter nuclei are required to calculate transition probabilities. Therefore we need to describe the level schemes of parent and daughter nuclei as accurate as possible. This is a difficult task because most effective interactions have trouble in dealing with nuclei in this region. A few β-decay schemes are shown below to demonstrate the feasibility of the new Hamiltonian and further discussion focused on these transitions are given.

Figure 2 shows the level schemes for ^{30}Na→^{30}Mg. We

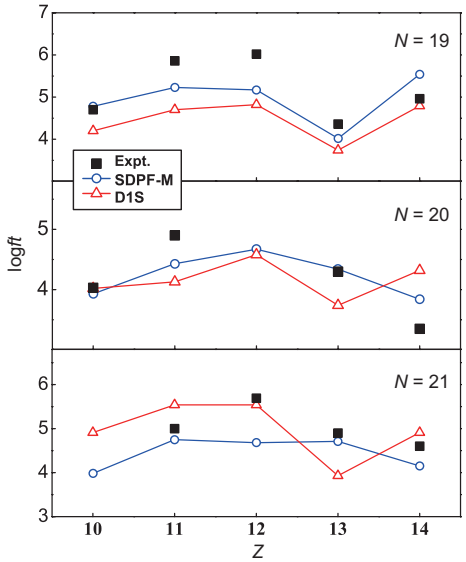

Figure 1 (Color online) Calculated logft of N=19-21 isotonic chains using the D1S-Gogny interaction and SDPF-M interactions are compared with experimental data are extracted using the NNDC On-Line Data Service[1)].

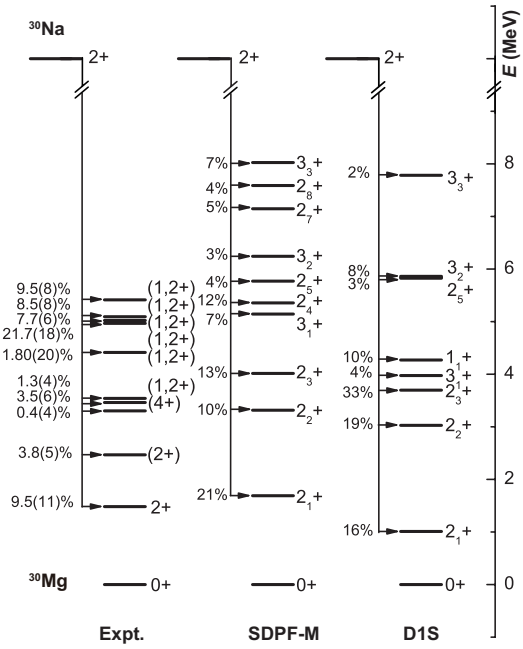

Figure 2 Experimental and theoretical β-decay schemes for ^{30}Na and its daughter ^{30}Mg. The branching ratio of each transition is listed on the left side of the level. Energy levels with uncertain spin and parity are either written as (J^π) or left blank. Experimental data are are extracted using the NNDC On-Line Data Service[1)].

2) R. Han, X. Q. Li, W. G. Jiang, et al. Northern boundary of the "Island of Inversion" and triaxiality in ^{34}Si, in preparation.

shall see that both D1S and SDPF-M interactions can reproduce the existing energy levels of the parent and daughter nuclei. The branching ratios of different transitions are quite dispersive and even the path with largest ratio can only occupy 20 to 30 percent. To interpret this dispersion, we compared the calculated wave functions of different excited states in ^{30}Mg. Results of both interactions reveal that they have similar configurations especially for the 2_n^+ states. The dispersion of the branching ratio is because of fair competition between these comparable states.

Furthermore, Figure 3 shows the level diagrams for ^{30}Mg→^{30}Al as a sequence of ^{30}Na→^{30}Mg. Both SDPF-M and Gogny calculations can provide reasonable branching ratios from the 0^+ g.s. in ^{30}Mg to different excited states in ^{30}Al. In experiment, the transition with the largest branching ratio 68(20)% is from the g.s. in ^{30}Mg to the first 1^+ excited state in ^{30}Al, whereas SDPF-M gives 95% and Gogny gives 71% for the corresponding path.

For ^{31}Ne→^{31}Na, there are no data for β-decay experiment to date. Shell-model calculations using the SDPF-M and D1S interactions are shown in Figure 4 to illustrate the feature of the transitions. Although the β-decay scheme seems complicated with a dozen transitions, one can still extract useful information from it. First, both theoretical calculations reproduce the low-lying spectra of ^{31}Na. As for the g.s. of the parent nucleus, its J^π is not yet confirmed in experiment and both the Gogny and SDPF-M calculations predict that the g.s. of ^{31}Ne is $3/2^-$. In addition, the same conclusion is drawn from the results of the two interactions that the transitions with the largest and second largest branching ratios are

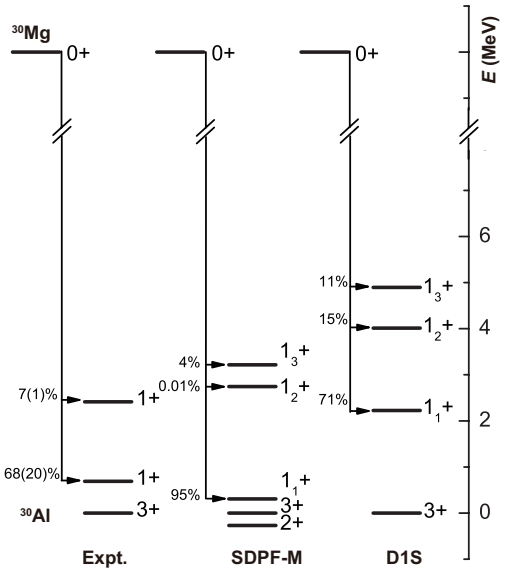

Figure 3 Experimental and theoretical β-decay schemes for ^{30}Mg and its daughter ^{30}Al. The branching ratio of each transition is listed on the left side of the level. Experimental data are extracted using the NNDC On-Line Data Service[1)].

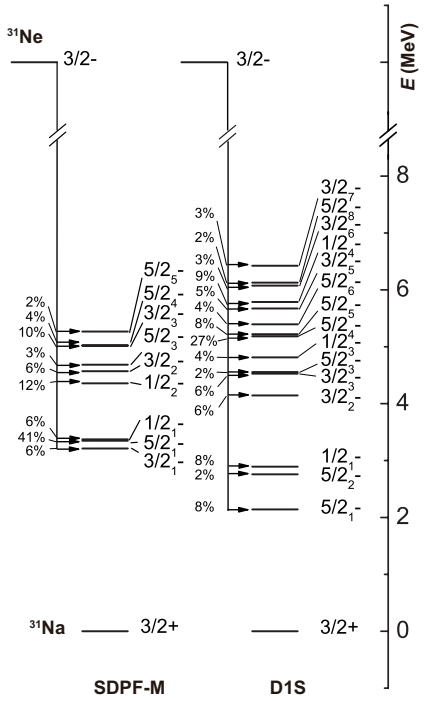

Figure 4 Theoretical β-decay schemes for ^{31}Ne and its daughter ^{31}Na. The branching ratio of each transition is listed on the left side of the level.

related to the $5/2^-$ and $1/2^-$ final states, respectively. With this information, we can better identify the different transitions of ^{31}Ne→^{31}Na when corresponding experimental data are avail able in the future. By analyzing all β-decay schemes in this region, we find that the D1S-Gogny shell-model Hamiltonian possesses advantage in describing the ground states of these nuclei so that it can also give good descriptions of transitions that are from g.s. to g.s..

4 Summary

In the present work, we investigated the properties of nuclei in and around the island of inversion through β-decay. A new cross-shell Hamiltonian is introduced and the TBMEs are deduced with the Gogny density-dependent interaction. Various properties including level schemes of the parent and daughter nuclei, logft, and branching ratios of transitions are calculated with the new Hamiltonian. Its results are compared with the SDPF-M calculations and experimental data. The good agreement between theoretical and experimental values suggests that the present Hamiltonian can provide useful information for the N=18-22, Z=10-14 nuclei with a unified Gogny interaction. By analyzing the logft value of these nuclei, we shall found a systematic structure evolution in N=19-21 isotonic chains and the saltation of logft for the Al isotopes. In addition, we presented the β-decay schemes of ^{30}Na→^{30}Mg, ^{30}Mg→^{30}Al and ^{31}Ne→^{31}Na to acquire more

detailed information on transitions and level schemes of the nuclei. Among these schemes, there are no experimental data for ^{31}Ne→^{31}Na transitions and the theoretical calculations are presented as predictions. In summary, the new Hamiltonian performs well for the island of inversion and maintains fine predictive power where experimental data are deficient.

This work was supported by the National Key Basic Research Program of China (Grant No. 2013CB834402), the National Natural Science Foundation of China (Grant Nos. 11235001, 11320101004, and 11575007), and the China-U.S. Theory Institute for Physics with Exotic Nuclei (CUSTIPEN) funded by the U.S. Department of Energy, Office of Science (Grant No. DE-SC0009971). We thank Prof. Utsuno and Otsuka (Department of Physics, University of Tokyo) for the SDPF-M interaction and C. X. Yuan (Sino-French Institute of Nuclear Engineering and Technology, Sun Yat-sen University) for fruitful discussions.

1 M. G. Mayer, Phys. Rev. **75**, 1969 (1949).
2 C. Thibault, R. Klapisch, C. Rigaud, A. M. Poskanzer, R. Prieels, L. Lessard, and W. Reisdorf, Phys. Rev. C **12**, 644 (1975).
3 G. Huber, F. Touchard, S. Bttgenbach, C. Thibault, R. Klapisch, H. T. Duong, S. Liberman, J. Pinard, J. L. Vialle, P. Juncar, and P. Jacquinot, Phys. Rev. C **18**, 2342 (1978).
4 C. Détraz, D. Guillemaud, G. Huber, R. Klapisch, M. Langevin, F. Naulin, C. Thibault, L. C. Carraz, and F. Touchard, Phys. Rev. C **19**, 164 (1979).
5 T. Motobayashi, Y. Ikeda, K. Ieki, M. Inoue, N. Iwasa, T. Kikuchi, M. Kurokawa, S. Moriya, S. Ogawa, H. Murakami, S. Shimoura, Y. Yanagisawa, T. Nakamura, Y. Watanabe, M. Ishihara, T. Teranishi, H. Okuno, and R. F. Casten, Phys. Lett. B **346**, 9 (1995).
6 E. K. Warburton, J. A. Becker, and B. A. Brown, Phys. Rev. C **41**, 1147 (1990).
7 X. Campi, H. Flocard, A. K. Kerman, and S. Koonin, Nucl. Phys. A **251**, 193 (1975).
8 E. Caurier, F. Nowacki, and A. Poves, Nucl. Phys. A **693**, 374 (2001).
9 Y. Utsuno, T. Otsuka, T. Mizusaki, and M. Honma, Nucl. Phys. A **704**, 50 (2002).
10 E. K. Warburton, and B. A. Brown, Phys. Rev. C **46**, 923 (1992).
11 B. A. Brown, and W. A. Richter, Phys. Rev. C **74**, 034315 (2006).
12 M. Honma, T. Otsuka, B. A. Brown, and T. Mizusaki, Phys. Rev. C **65**, 061301 (2002).
13 B. H. Wildenthal, Prog. Particle Nucl. Phys. **11**, 5 (1984).
14 E. K. Warburton, and J. A. Becker, Phys. Rev. C **40**, 2823 (1989).
15 J. Dechargé, and D. Gogny, Phys. Rev. C **21**, 1568 (1980).
16 G. X. Dong, X. B. Wang, and S. Y. Yu, Sci. China-Phys. Mech. Astron. **58**, 112004 (2015).
17 W. Y. Liang, C. F. Jiao, F. R. Xu, and X. M. Fu, Sci. China-Phys. Mech. Astron. **59**, 692012 (2016).
18 A. C. Morton, P. F. Mantica, B. A. Brown, A. D. Davies, D. E. Groh, P. T. Hosmer, S. N. Liddick, J. I. Prisciandaro, H. Schatz, M. Steiner, and A. Stolz, Phys. Lett. B **544**, 274 (2002).
19 V. Tripathi, S. L. Tabor, P. Bender, C. R. Hoffman, S. Lee, K. Pepper, M. Perry, P. F. Mantica, J. M. Cook, J. Pereira, J. S. Pinter, J. B. Stoker, D. Weisshaar, Y. Utsuno, and T. Otsuka, Phys. Rev. C **77**, 034310 (2008).
20 F. Rotaru, F. Negoita, S. Grévy, J. Mrazek, S. Lukyanov, F. Nowacki, A. Poves, O. Sorlin, C. Borcea, R. Borcea, A. Buta, L. Cáceres, S. Calinescu, R. Chevrier, Z. Dombrádi, J. M. Daugas, D. Lebhertz, Y. Penionzhkevich, C. Petrone, D. Sohler, M. Stanoiu, and J. C. Thomas, Phys. Rev. Lett. **109**, 092503 (2012).
21 T. Zidar, in *Investigation of the nuclear structure of ^{33}Al through beta-decay of ^{33}Mg to probe the island of inversion: Proceedings of APS Division of Nuclear Physics Meeting* (APS, Vancouver, 2016).
22 B. H. Wildenthal, Prog. Particle Nucl. Phys. **11**, 5 (1984).
23 B. A. Brown, and W. A. Richter, Phys. Rev. C **74**, 034315 (2006).
24 B. Rubio, and W. Gelletly, *The Euroschool Lectures on Physics with Exotic Beams* (Springer, Berlin Heidelberg, 2009), pp. 99-151.
25 C. Détraz, D. Guillemaud, G. Huber, R. Klapisch, M. Langevin, F. Naulin, C. Thibault, L. C. Carraz, and F. Touchard, Phys. Rev. C **19**, 164 (1979).
26 Y. Utsuno, T. Otsuka, T. Mizusaki, and M. Honma, Phys. Rev. C **60**, 054315 (1999).
27 Y. Utsuno, T. Otsuka, T. Glasmacher, T. Mizusaki, and M. Honma, Phys. Rev. C **70**, 044307 (2004).
28 J. Dechargé, and D. Gogny, Phys. Rev. C **21**, 1568 (1980).
29 R. W. Ibbotson, T. Glasmacher, B. A. Brown, L. Chen, M. J. Chromik, P. D. Cottle, M. Fauerbach, K. W. Kemper, D. J. Morrissey, H. Scheit, and M. Thoennessen, Phys. Rev. Lett. **80**, 2081 (1998).
30 H. Scheit, T. Glasmacher, B. A. Brown, J. A. Brown, P. D. Cottle, P. G. Hansen, R. Harkewicz, M. Hellström, R. W. Ibbotson, J. K. Jewell, K. W. Kemper, D. J. Morrissey, M. Steiner, P. Thirolf, and M. Thoennessen, Phys. Rev. Lett. **77**, 3967 (1996).
31 B. A. Brown, and B. H. Wildenthal, Annu. Rev. Nucl. Part. Sci. **38**, 29 (1988).
32 T. T. S. Kuo, and G. E. Brown, Nucl. Phys. A **114**, 241 (1968).
33 D. J. Millener, and D. Kurath, Nucl. Phys. A **255**, 315 (1975).
34 J. F. Berger, M. Girod, and D. Gogny, Comp. Phys. Commun. **63**, 365 (1991).